

Characterization of GNSS Receiver Position Errors for User Integrity Monitoring in Urban Environments

Khairol Amali Bin Ahmad, Mohamed Sahmoudi, Christophe Macabiau

► **To cite this version:**

Khairol Amali Bin Ahmad, Mohamed Sahmoudi, Christophe Macabiau. Characterization of GNSS Receiver Position Errors for User Integrity Monitoring in Urban Environments. ENC-GNSS 2014, European Navigation Conference, Apr 2014, Rotterdam, Netherlands. <hal-01160130>

HAL Id: hal-01160130

<https://hal-enac.archives-ouvertes.fr/hal-01160130>

Submitted on 4 Jun 2015

HAL is a multi-disciplinary open access archive for the deposit and dissemination of scientific research documents, whether they are published or not. The documents may come from teaching and research institutions in France or abroad, or from public or private research centers.

L'archive ouverte pluridisciplinaire **HAL**, est destinée au dépôt et à la diffusion de documents scientifiques de niveau recherche, publiés ou non, émanant des établissements d'enseignement et de recherche français ou étrangers, des laboratoires publics ou privés.

Characterization of GNSS Receiver Position Errors for User Integrity Monitoring in Urban Environments

K.A. Bin Ahmad¹, M. Sahmoudi² and C. Macabiau³

¹ISAE, University of Toulouse, France, Khairol-amali.AHMAD@etu.isae.fr

²ISAE, University of Toulouse, France, mohamed.sahmoudi@isae.fr

³ENAC, University of Toulouse, Toulouse, France,

Abstract: The characterization of GNSS position errors in urban environments is an important issue for integrity monitoring and classification of receivers' performance. However, these errors are not observable directly by the receiver, therefore RAIM methods use statistics based on the pseudorange residuals (i.e. observable errors). In this work, we focus on the modelling and analysis of navigation errors in the position-domain rather than individual range-domain errors that are difficult to model in urban environments due to multipath and non-line-of-sight (NLOS) signals. Using a trajectory of reference we compute the horizontal position errors (HPE) and its non-parametric distribution function given by the empirical Cumulative Distribution Function (CDF). According to the results, we observe that these errors have a heavy-tailed distribution, and then we propose to fit the empirical CDF with the CDF of the generalized Pareto distribution (GPD). We use an inflated version of the fitted Pareto model to overbound the CDF of the HPE for the calculation of Horizontal Protection Level (HPL), i.e., bounding the radial position errors.

BIOGRAPHIES

Khairol Amali bin Ahmad obtained a BSc in Electrical Engineering in 1992 from the United States Military Academy, West Point and an MSc in Military Electronic Systems Engineering in 1999 from Cranfield University. Since 2011, he is a PhD student at the French Institute of Aeronautics and Space (ISAE) working on reliability monitoring aspects of GNSS aided navigation systems for land vehicle applications in harsh environment.

Mohamed Sahmoudi received a PhD in signal processing and communications from Paris Sud University and Telecom Paris in 2004, and an M. S. degree in statistics from Pierre and Marie Curie University in 2000. During his PhD, he was an assistant lecturer at Ecole Polytechnique, then a lecturer at Paris Dauphine University. From 2005 to 2007, he was a postdoc researcher on GPS signal processing at Villanova University, PA, USA. In August 2007, he joined the ETS School of Engineering at Montreal, Canada, to work on GNSS RTK for precise positioning. In December 2009, he became an associate professor at the French Institute of Aeronautics and Space (ISAE), Toulouse, France. His research interest includes weak multi-GNSS signals processing, multipath mitigation and multi-sensor fusion.

Christophe Macabiau graduated as an electronics engineer in 1992 from the ENAC (Ecole Nationale de l'Aviation Civile) in Toulouse, France. Since 1994, he has been working on the application of satellite navigation techniques to civil aviation. He received his PhD in 1997 and has been in charge of the signal processing lab of ENAC from 2000 to 2012, where he also started dealing with navigation techniques for urban navigation. He is currently the head of the TELECOM lab of ENAC, which includes research groups on signal processing and navigation, electromagnetics and data communication networks.

1 INTRODUCTION

The GNSS positioning services for land navigation has grown in popularity and usefulness that they are poised to be receiving more demands from users. These existing terrestrial applications together

with many more potential services cover a broad range of applications such as location based charging, pay-as-you-drive (PAYD) road charging and geo-localization reporting (Giraud, 2013). In addition, the applications for Advance Driver Assistance System (ADAS) such as lane keeping, collision avoidance and so forth also make use of the GNSS positioning system (Lu, 2005). Since many of the services involve financial, legal and potentially safety-of-life repercussions, these applications would need compliance with safety and reliability requirements. However, to foster innovation and further expedite the development for the land navigation applications, a lot of effort is needed to achieve the technical and regulation requirements. One of the imperative and pressing goals to be achieved is the standardization of the terrestrial GNSS-based location systems (Giraud, 2013).

It should be highlighted that, in these land based applications, the GNSS receiver is normally a sub-system for providing positioning, velocity and time (PVT) information that would be used as subsequent inputs by the next module in the application system as a whole. In fact, the GNSS is not the only technology involves in the positioning module when hybrid solution is implemented. In such case, the GNSS technology is complemented by other sensors, such as inertial or odometric, in order to improve the performance of the PVT solution. Figure 1 shows a generic structure of the concept. Therefore, there is a need to choose a suitable receiver type and to know its minimum performances in order to meet the final application's requirement at the user level (Aichhorn, 2011, Cosmen-Schortmann, 2009). For this purpose, the characterization of positioning error is needed to provide the final user with the level of confidence in the application which uses the level of confidence of the GNSS solution. In this paper, we address the problem of GNSS position error characterization.

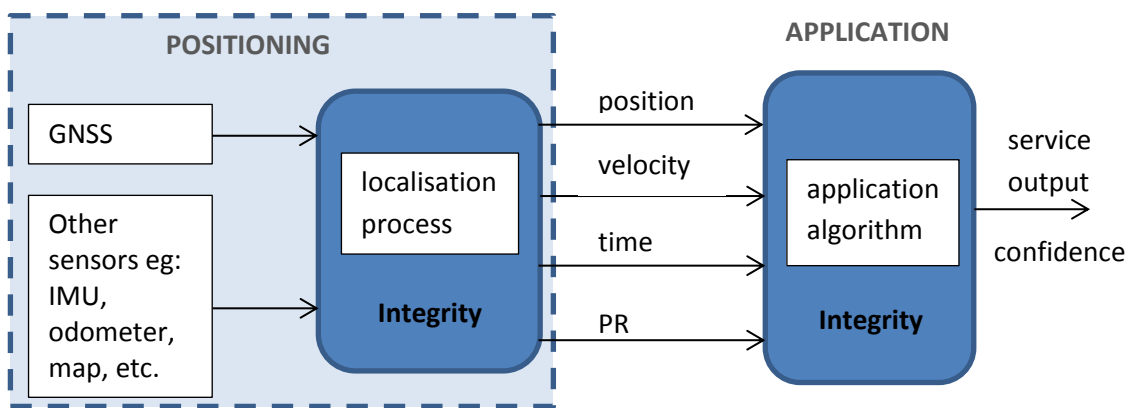


Figure 1. Generic architecture for land application system

In principle, GNSS positioning depends on the quality of the pseudorange measurements and the satellite geometry. However, for land navigation, characterizing positioning error of a receiver is not a simple matter because the positioning quality depends on the receiver's operating environment, the type and characteristic of receiver (such as its inside signal processing, stand-alone or hybrid), the positioning algorithms and the mitigation techniques being used. Usually, the user does not have access to these receiver design parameters. However, the positioning performance of a stand-alone GNSS receiver would probably be less robust as compared to the hybrid multi-sensor type receiver.

Due to the various affecting factors, a GNSS receiver performance cannot be predicted without knowing under which conditions it will be operated. Therefore, the receiver performance characteristic can only be defined statistically and must also be categorized in relation to the various operational environments which are relevant to the intended applications.

To assess the receiver performance characteristic, the work in this paper aim to characterize the Horizontal Position Error (HPE) in an urban environment. It is well known that buildings and natural geographical obstacles reduce the visibility of satellites and add different kind of bias in the pseudorange measurements due to multipath and non-line of sight (NLOS) reflections, producing a position error of ten to hundreds of meters. While there have been various works on characterizing and modelling the measurement/pseudorange error in urban environments (Spangenberg, 2008, Viandier, 2008), very few works exist in the open publications literature on the positioning error characterization and modelling.

In this work, we focus on the positioning error characterization because modelling the effect of NLOS on the measurements is quite difficult and does not guarantee the characterization of the final position error (Groves, 2012). In fact, different PR errors on the PR may combine between them to produce new kind of errors on the position solution. For example, it has been observed in the Satellite-based augmentation system (SBAS) literature that errors terms between different satellites may be correlated and finally challenged the standard protection level (xPL) methods based on the non-correlation assumption (Langel, 2012). Hence, the availability of a statistical characterization of the position error is also very useful for computing integrity indicators. Since there are biases in urban environment due to multipath and NLOS, we need to take into account of these errors in the position integrity monitoring (Sayim, 2003, Walter, 2004, Rife, 2005). One way to deal with biases is through overbounding technique.

The common approach to overbounding in the aviation sector is to use zero mean Gaussian distribution and then inflate its variance to accommodate additional errors or biases in the actual distribution. While the errors and biases model in the aviation sector is well developed, in urban environments, the NLOS biases are complex and difficult to model. Therefore, we adopt a direct position-domain approach for integrity monitoring.

There are two related parts in this work. In the first part, the HPE distribution is obtained empirically and fitted to Rayleigh and Pareto distributions depending on the receiver environment. We observed that the Pareto distribution has a better fit to the HPE in urban and deep urban environment while Rayleigh distribution is better in the open sky areas. In the second part, the methodology of direct position domain CDF overbounding with Pareto distribution is applied to consider the biases due to NLOS and multipath in the urban environment.

2 HORIZONTAL POSITION ERROR REPRESENTATION

In this work, the characterization of the receiver's position error using the HPE distribution is obtained from the position error in the north and the east components. The errors are computed based on the difference between measured positions and referenced true positions:

$$\begin{aligned} \mathbf{E}_{pos} &= \mathbf{X}_{measured} - \mathbf{X}_{ref} \\ \text{where } \mathbf{E}_{pos} &= \begin{bmatrix} E_{east} \\ E_{north} \end{bmatrix} \end{aligned} \quad (1)$$

Due to the 2D nature of the horizontal error (north and east components), the HPE can be represented as a radial error and defined as:

$$HPE = \sqrt{E_{east}^2 + E_{north}^2} \quad (2)$$

2.1 HPE distribution in open sky

In open sky environments, in general the measured PR errors tend to be normally distributed. In estimating the receiver position using the measured PRs, these Gaussian PR errors are combined and propagated to the position domain via the linear estimation matrix to also form Gaussian distributed errors, i.e. the E_{east} and E_{north} also tend to be Gaussian distributed. Theoretically, assuming ideal conditions where the E_{east} and E_{north} distributions are also zero mean and independent, the distribution of their norm, which is the HPE, would be Rayleigh distributed.

Based on this assumption, we computed the PDF and CDF of the HPE using the empirical data as plotted in Figure 2. The HPE has been computed using the difference between the measured position of the receiver and reference solution. The HPE distribution is then fitted to a Rayleigh distribution, where the CDF of a Rayleigh distribution is given by (Walck, 2007):

$$CDF_{Rayleigh} = 1 - e^{-x^2/2\sigma^2} \quad (3)$$

and σ is the scale parameter of the distribution.

2.2 HPE distribution in urban environments

In the case for urban environments, it has been shown that the distributions of the PR errors are likely non-Gaussian due to the biases from the multipaths and NLOS signal propagations. Even though according to the central limit theorem that the non-Gaussian ranging errors would cause the position-domain distribution tends towards a Gaussian distribution as the number of ranging measurements increases, such situation is not probable in the urban environments because the number of visible satellites tend to be limited due to blockage from buildings and other infrastructures. Because of these reasons, we perform the curve fitting for the HPE in the urban environment using the Pareto distribution.

In general, Pareto is suitable for distributions with heavy tail, such as the case of the position error in urban settings where there are plenty of large errors with small probabilities. The classical Pareto distribution (also known as Pareto distribution type I) has a tail function that describes the probability that X , as a random variable, is greater than some number x . This function is given by (Johnson, 1994):

$$\bar{F}(x) = \Pr(X > x) = \left(\frac{x}{\sigma}\right)^{-\alpha}, \quad x \geq \sigma \quad (4)$$

where σ is the scale parameter and α is a shape parameter. From this definition, it can be seen that $\bar{F}(x) = 1 - CDF_{ParetoI}$. Therefore, the algebraically decreasing CDF of Pareto is given by:

$$CDF_{ParetoI} = 1 - \left(\frac{x}{\sigma}\right)^{-\alpha} \quad \text{for } x \geq \sigma \quad (5)$$

The generalized Pareto distribution (GPD) has a CDF expressed as:

$$F(x) = \begin{cases} 1 - \left(1 + \frac{\xi(x-\mu)}{\sigma}\right)^{-\frac{1}{\xi}} & \text{for } \xi \neq 0 \\ 1 - \exp\left(-\frac{x-\mu}{\sigma}\right) & \text{for } \xi = 0 \end{cases} \quad (6)$$

The probability distribution of the GPD is given by:

$$PDF_{GPD} = \frac{1}{\sigma} \left(1 + \xi \frac{(x-\mu)}{\sigma}\right)^{-\frac{1}{\xi}-1} \quad (7)$$

For added flexibility, the generalized Pareto distribution has 3 parameters which are the scale σ , the shape ξ and the location μ . The generalized Pareto distribution is used in this work to implement the curve fitting to the empirical HPE distributions using MATLAB. The plots are in Figure 3.

2.3 Along-street and across-street error distributions in urban environment

In the urban environment, apart from the radial HPE characterization, the position errors are also observed in terms of ‘‘along the street’’ and ‘‘across the street’’ errors. For some land navigation applications (such as lane keeping), this along street (forward) errors and across street (lateral) errors characterization could be a more suitable alternative to the HPE in the radial form. The geometric configuration affects differently for these errors in two directions depending on the street orientation in space.

In order to convert the E_{east} and E_{north} to E_{fwd} and $E_{lateral}$, E_{pos} is multiplied with a rotational matrix R (Goldstein, 2002). Therefore,

$$\mathbf{E}_{fwd_lat} = \begin{bmatrix} E_{fwd} \\ E_{lateral} \end{bmatrix} = \mathbf{R} \cdot \mathbf{E}_{pos} \quad (8)$$

where,

$$\mathbf{R} = \begin{bmatrix} \cos \theta & \sin \theta \\ -\sin \theta & \cos \theta \end{bmatrix}, \quad \theta = \text{atan2}(\text{ref}_{\Delta N}, \text{ref}_{\Delta E})$$

$\text{ref}_{\Delta E}$ is the distance of 2 consecutives referenced position in the East direction

$\text{ref}_{\Delta N}$ is the distance of 2 consecutives referenced position in the North direction

Their PDFs and CDFs plots are given in Figure 4. For linear estimation of the position error E_{pos} in Eq. (1), the variance matrix is,

$$\boldsymbol{\Sigma} = \begin{pmatrix} \sigma_E^2 & \sigma_{EN} \\ \sigma_{NE} & \sigma_N^2 \end{pmatrix}$$

Therefore in matrix form, it follows that:

$$HPE = \|\mathbf{E}_{pos}\| = \sqrt{\mathbf{E}_{pos}^T \boldsymbol{\Sigma}^{-1} \mathbf{E}_{pos}} \quad (9)$$

and

$$\|\mathbf{E}_{pos}\|^2 = \mathbf{E}_{pos}^T \boldsymbol{\Sigma}^{-1} \mathbf{E}_{pos} = r^2 \quad (10)$$

which describes the border line of an ellipse. Through eigenvalue decomposition, (Tiberius, 2008) shows that a positive definite and symmetric variance matrix $\boldsymbol{\Sigma}$ can be equated to

$$\boldsymbol{\Sigma} = \mathbf{U}\boldsymbol{\Lambda}\mathbf{U}^T \quad (11)$$

where diagonal matrix $\boldsymbol{\Lambda}$ contains positive eigenvalues of $\boldsymbol{\Sigma}$ (assume $\lambda_1 \geq \lambda_2$) and orthogonal matrix \mathbf{U} contains the corresponding eigenvectors u_1 and u_2 which dictate the direction of the principal axes of the ellipse. The length of the semi-major axis is $\sqrt{\lambda_1}r$ and the length of the semi-minor axis is $\sqrt{\lambda_2}r$. In the elaboration, it is shown that when

$$\mathbf{v} = \mathbf{U}^T \mathbf{E}_{pos} \quad (12)$$

Then,

$$r^2 = \|\mathbf{E}_{pos}\|^2 = \mathbf{v}^T \boldsymbol{\Lambda}^{-1} \mathbf{v} \quad (13)$$

In Eq. (12), the position errors are projected in the direction of the semi-major axis u_1 and the semi-minor axis u_2 of the error ellipse.

3 POSITIONING INTEGRITY

3.1 CDF Overbounding

Error ellipse is related to the positioning confidence level or integrity by the HPE cumulative distribution function. Once the CDF of the HPE is estimated, we can compute a protection radius of integrity from the inverse of the CDF.

$$F_R(R_{emp}) = Prob(\text{position error} \leq R_{emp}) = P_b \quad (14)$$

$$\rightarrow R_{emp} = F_R^{-1}(P_b) = \text{Inverse CDF}(P_b) \quad (15)$$

However, the true HPE cannot be known without knowing a reference position. Therefore, in navigation, an overbounding Horizontal Protection Level (HPL) is usually used. Overbounding refers to the process of replacing the actual error distribution by a simplified conservative model, with the objective of having enough margin to take into account the risk of non-modelled errors. Conservative models of errors is said to overbound the actual error distribution when for a given level of probability, the magnitude of the error of the error model is bigger than what can be found in the actual data (Osechas, 2013).

$$G_o(x) \leq G_a(x), \quad \forall x \geq 0 \quad (16)$$

where $G_o(x)$ is the overbounding CDF and $G_a(x)$ is the actual CDF.

Therefore, the CDF of HPE provides a base for calculating the integrity or designing the Horizontal Protection Level (HPL) depending on the "risk tolerance" of the application. The protection level (PL) is defined by inverting an overbound and evaluating the inverted function at an allowed fault probability (probability of hazardous misleading information, P_{HMI}). The magnitude of the PL depends on the form of the overbounding CDF, G_o . As an example, for a zero mean Gaussian error characterized by a Gaussian CDF, PL can be calculated by $xPL = A_o \sigma_o$. For HPL, (RTCA, 2006) gives the formula as:

$$HPL = \begin{cases} K_{H,NPA} d_{major} \\ K_{H,PA} d_{major} \end{cases} \quad (17)$$

with

$$d_{major} = \sqrt{\frac{d_{east}^2 + d_{north}^2}{2} + \sqrt{\left(\frac{d_{east}^2 - d_{north}^2}{2}\right)^2 + d_{EN}^2}}$$

$$d_{east}^2 = \sum_{i=1}^N S_{east,i}^2 \sigma_i^2$$

$$d_{north}^2 = \sum_{i=1}^N S_{north,i}^2 \sigma_i^2$$

$$d_{EN}^2 = \sum_{i=1}^N S_{east,i} S_{north,i} \sigma_i^2$$

where N is the number of visible satellites, σ_i^2 is the PR error variance of the i -th satellite, and S is the pseudo-inverse matrix of the geometry matrix to transform the PR errors to position errors according to the least square method:

$$\mathbf{z} = \mathbf{G}\mathbf{x} + \boldsymbol{\varepsilon},$$

$$\hat{\mathbf{x}} = \min_x \|\mathbf{z} - \mathbf{G}\mathbf{x}\|^2,$$

$$\hat{\mathbf{x}} = (\mathbf{G}^T \mathbf{G})^{-1} \mathbf{G}^T \mathbf{z} = \mathbf{S}\mathbf{z},$$

where \mathbf{z} is PR measurement vector, \mathbf{x} is position vector, \mathbf{G} is geometry matrix, $\boldsymbol{\varepsilon}$ position error vector and \mathbf{S} is pseudo-inverse matrix.

In presence of bias, the PL can be formulated as a sum of nominal component plus a bias component:

$$\begin{aligned} PL &= PL_o + PL_b \\ PL &= A_o \sigma_o + PL_b \end{aligned} \quad (18)$$

Let μ_i be the bias of each PR, PL_b is the total bias expressed as:

$$PL_b = \sum_{i=1}^N S_i \mu_i$$

In civil aviation, specific sources and effects of the bias have been considered and modelled (Rife, 2005). In urban environment, the biases are mainly due to NLOS and multipath reception which are difficult to model, then it is very difficult to come up with an expression of PL_b .

The common method for generating the PL assumes a zero-mean Gaussian error model. However, the actual error distribution is not necessarily zero-mean Gaussian. In order to ensure that the Gaussian model overbound the true error, its variance is usually inflated to cover other kind of errors (bias from satellite, etc.) A series of work such as by (DeCleene, 2000) and (Rife, 2004a) had tackled on the Gaussian overbounding issues. The overbound, unlike the actual error distribution, need not integrate to a total probability mass of one. In excess-mass CDF (EMC), bound can be defined with a limiting value above one (Rife, 2004b):

$$K = \lim_{x \rightarrow \infty} G_o(x) \geq 1 \quad (19)$$

where K is the mass parameter and $G_o(x)$ is the overbounding CDF.

Most additional errors from satellite, environment or the processing algorithm have large amplitude with low probabilities which yield to a heavier tail of the actual error distribution than the Gaussian one. When dealing with non-Gaussian tail or 'heavy tail' error distribution, (Shively and Braff, 2000) derived the sigma inflation factors by using a model of Gaussian core and Laplacian tails. (Rife, 2004c) had proposed Gaussian core and Gaussian sidelobes to mitigate overconservatism when bounding heavy tails.

3.2 Direct position domain overbounding using generalized Pareto CDF

Overbounding using the position domain method is an alternative to the range domain method which monitors each pseudorange measurement individually. The position domain method is able to

produce tighter PL and therefore increase availability because the conservatism assumptions were applied only to the position-domain error distribution model and not to each individual range-domain error distribution model (Lee, 2009).

The concept of position domain overbounding is elaborated in the works of (Ober, 2004, Rife, 2005, Lee, 2009, Osechas, 2013). Furthermore, (Osechas, 2013) highlighted the main difference of direct position domain overbounding as compared to the conventional indirect position domain overbounding approach is that in the direct approach, the overbounds are calculated by inspecting error data directly, without transforming the errors from the range domain to the position domain.

In this paper, we combine the direct position domain and the CDF overbounding concepts. Then we use the Pareto distribution to directly overbound the HPE CDF for positioning in the urban environments. Based on the HPE CDF obtained from empirical data processed in this work in the previous section, the generalized Pareto distribution showed a good fitting with the HPE CDF in urban environment. From the definition of the CDF overbounding, the overbounding CDF must cover larger errors than the actual data for a given level of probability or conversely, the overbounding CDF has lower probability than the actual CDF for the same error value (Tiberius, 2008). This condition can be achieved by adjusting the Pareto distribution in relation to the HPE using the GPD parameters. Using the GPD CDF to overbound the HPE CDF,

$$G_o(x) = CDF_{GPD} = 1 - \left[1 + \xi \left(\frac{x-\mu}{\sigma}\right)\right]^{-\frac{1}{\xi}} \text{ for } x \geq \mu \quad (20)$$

The scale parameter σ affects the size and slope of the distribution. The shape parameter ξ affect the shape of the tail of the distribution and the location parameter μ is related to the value of x when the CDF = 0. To overbound the HPE by CDF_{GPD} , we proceed by shifting the location parameter. Indeed, if we fix the ξ value, then,

$$1 - \left[1 + \xi \left(\frac{x - \mu_o}{\sigma}\right)\right]^{-\frac{1}{\xi}} \geq 1 - \left[1 + \xi \left(\frac{x - \mu_1}{\sigma}\right)\right]^{-\frac{1}{\xi}}$$

where μ_1 is the new value to achieve overbound. After simplification of the formula, we obtain:

$$\begin{aligned} 1 - \frac{\xi \mu_1}{\sigma} &\leq 1 - \frac{\xi \mu_o}{\sigma} \\ \rightarrow \frac{\xi \mu_1}{\sigma} &\geq \frac{\xi \mu_o}{\sigma} \quad \rightarrow \mu_1 \geq \mu_o. \end{aligned}$$

Once the generalized Pareto CDF overbound the CDF of the HPE, the Horizontal Protection Level can be calculated from its inverse. Given,

$$CDF_{GPD} = 1 - \left[1 + \xi \left(\frac{x-\mu}{\sigma}\right)\right]^{-\frac{1}{\xi}} = Prob(\text{position error} \leq x) \quad (21)$$

Let R_p be the PL error. Equating the CDF to integrity probability, P_B ,

$$1 - \left[1 + \xi \left(\frac{R_p - \mu}{\sigma}\right)\right]^{-\frac{1}{\xi}} = (1 - P_{HMI}) = P_B \quad (22)$$

To obtain the HPL, we solve for R_p ,

$$\begin{aligned} \left[1 + \xi \left(\frac{R_p - \mu}{\sigma}\right)\right]^{-\frac{1}{\xi}} &= 1 - P_B \\ \frac{-1}{\xi} \ln \left[1 + \xi \left(\frac{R_p - \mu}{\sigma}\right)\right] &= \ln(1 - P_B) \\ \ln \left[1 + \xi \left(\frac{R_p - \mu}{\sigma}\right)\right] &= -\xi \ln(1 - P_B) \\ \left[1 + \xi \left(\frac{R_p - \mu}{\sigma}\right)\right] &= (1 - P_B)^{-\xi} \end{aligned}$$

$$\xi \left(\frac{R_p - \mu}{\sigma} \right) = (1 - P_B)^{-\xi} - 1$$

Hence,

$$HPL = R_p = \frac{\sigma}{\xi} [(1 - P_B)^{-\xi} - 1] + \mu \quad (23)$$

For ground positioning, the HPL can be defined as a bound on the HPE with a probability derived from the integrity requirements. Thus we focus in this work on bounding the HPE directly in the position domain. The plot of the overbounding GPD with $\mu = 1$ and $\sigma = 6$ is given in Figure 5.

The following table summarizes the proposed methodology for bounding the HPE in presence of multipath and NLOS biases.

Table 1. Proposed methodology for bounding HPE in presence of multipath and NLOS

| | |
|----------------|---|
| <u>Step 1:</u> | Computation of the ECDF using the reference trajectory |
| <u>Step 2:</u> | Curve fitting of the ECDF with generalized Pareto distribution (GPD) <ul style="list-style-type: none"> - Estimation of GPD parameter from data. - Adjust GPD parameter to achieve GPD CDF overbounding of ECDF |
| <u>Step 3:</u> | Compute HPL |

4 DATA COLLECTION AND EXPERIMENTAL SETUP

The data is gathered in Toulouse downtown area where the receivers are used to measure the position. The receivers used in this work are the Ublox 4T, Novatel and Ublox 6T receivers. Ublox 4T and Novatel used the same trajectory but Ublox 6T used a different trajectory. In order to obtain the positioning errors, the measured positions are compared along the trajectories to the reference positions obtained from a high grade navigation system (SPAN Novatel GPS/iMAR IMU).

5 RESULTS AND DISCUSSIONS

5.1 Rayleigh distribution curve fitting for HPE CDF in open sky environment

Figure 2a shows the PDF and the CDF of the HPE of the Ublox 4T receiver in the open sky environment. The histogram is obtained from the empirical data and the Rayleigh tracing is included to compare its form against the HPE PDF where we can see close resemblance. The PDF shows the deviation of the HPE to be around 16 meters range. From the CDF plot, it can be seen that the HPE has quite good accuracy of about 3 meters at 90% confidence, 4 meters at 95% confidence and 5 meters at 99% confidence level. When fitting the HPE CDF with Rayleigh and generalized Pareto CDFs, it appears that in the case of open sky, the Rayleigh CDF has a better fitting. This can be related to the fact that Pareto is suitable for distribution with heavy tail.

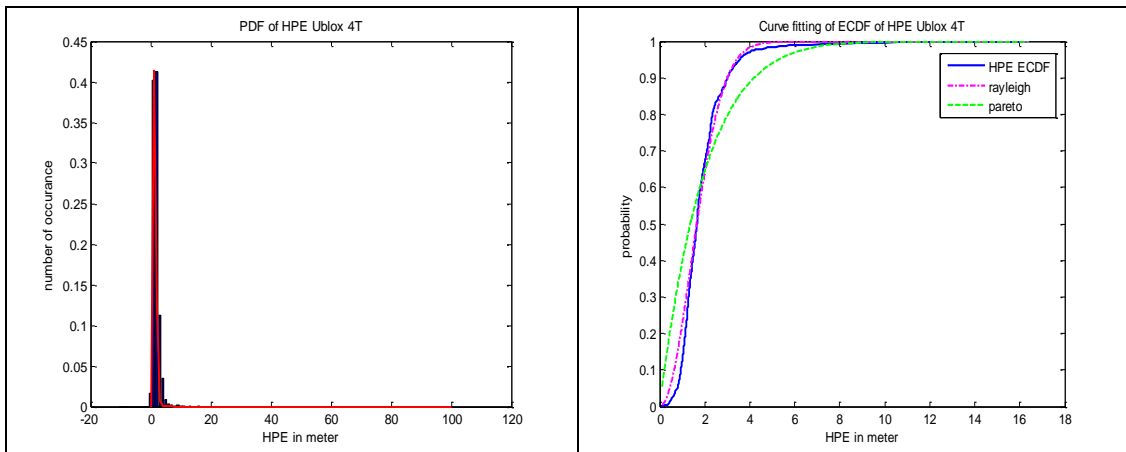


Figure 2a. PDF and CDF in open sky area

In the Q-Q plot in Figure 2b, it can be seen also that the Rayleigh distribution has a better fitting with the HPE CDF when compared to Pareto distribution.

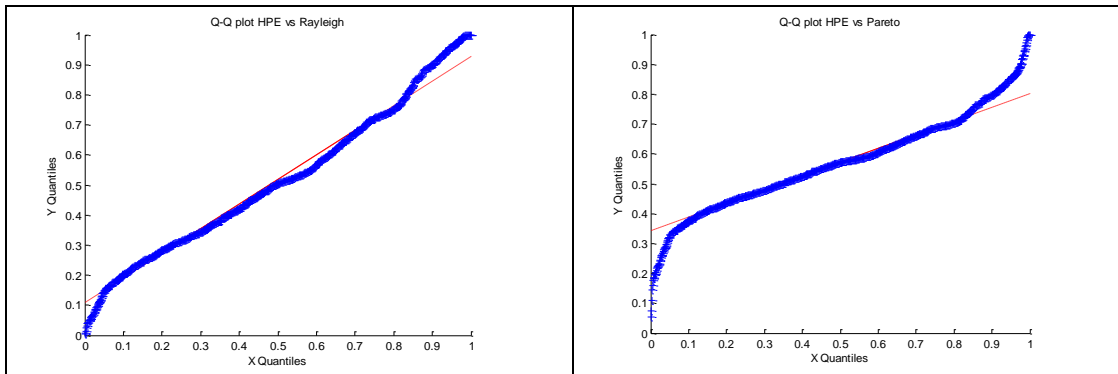


Figure 2b. Q-Q plots comparing HPE vs Rayleigh Distribution and HPE vs Pareto Distribution (open sky)

5.2 Generalized Pareto distribution curve fitting for HPE CDF in urban environment

5.2.1 Ublox 4T receiver

Figure 3a shows the PDF of the HPE of the Ublox 4T receiver in the urban environment. The PDF shows a distribution that has a deviation of about 40 meters, indicating a wider error range than in the open sky area. Comparing the HPE PDF against a Rayleigh distribution tracing (left figure), it can be seen that the two distributions are significantly different while the comparison with generalized Pareto tracing (right figure) shows a better fitting of the heavy tail.

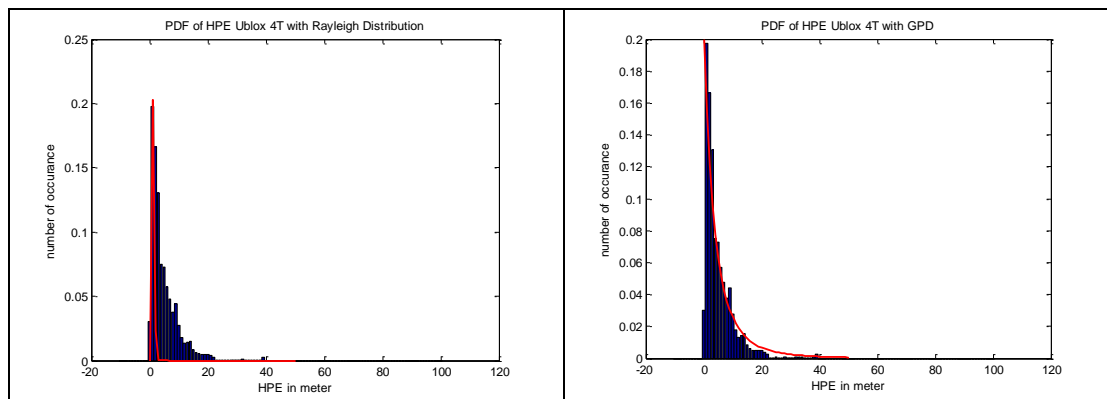


Figure 3a. PDF comparison in urban environment

From the HPE CDF in Figure 3b, the accuracy of the positioning is about 11 meters at 90% confidence and 15 meters at 95% confidence. This increase of error and the change of distribution shape are mainly due to the biases from multipath and NLOS in urban environment. In term of curve fitting, the CDF plots show that the GDP has better fitting than Rayleigh.

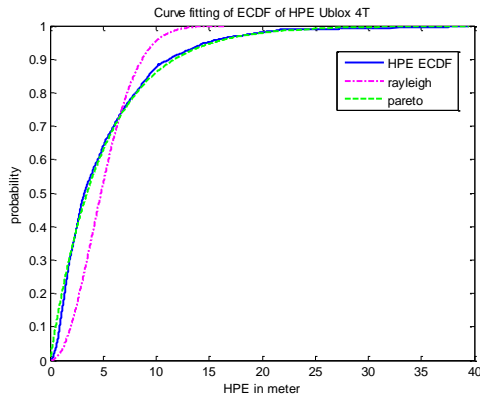


Figure 3b. CDF in urban environment

In the Q-Q plots of Figure 3c, it can be observed also that the Pareto distribution has a better fitting with the HPE than the Rayleigh distribution when in urban environment.

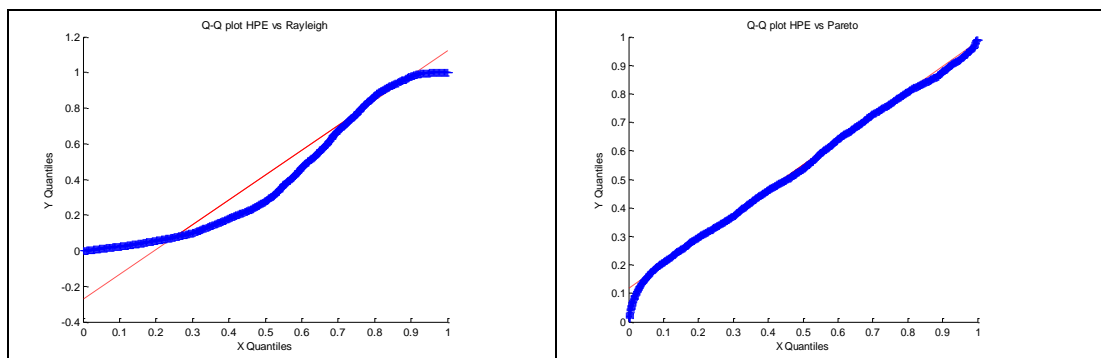


Figure 3c. Q-Q plots comparing HPE vs Rayleigh Distribution and HPE vs Pareto Distribution (urban environment)

5.2.2 Novatel receiver

Figure 3d shows the curve fitting of the HPE CDF for Novatel receiver in urban environment. In this case, the generalized Pareto distribution also has a good fitting as compared to the Rayleigh distribution, as can be seen in the CDF plots, and the Q-Q plot of the GPD.

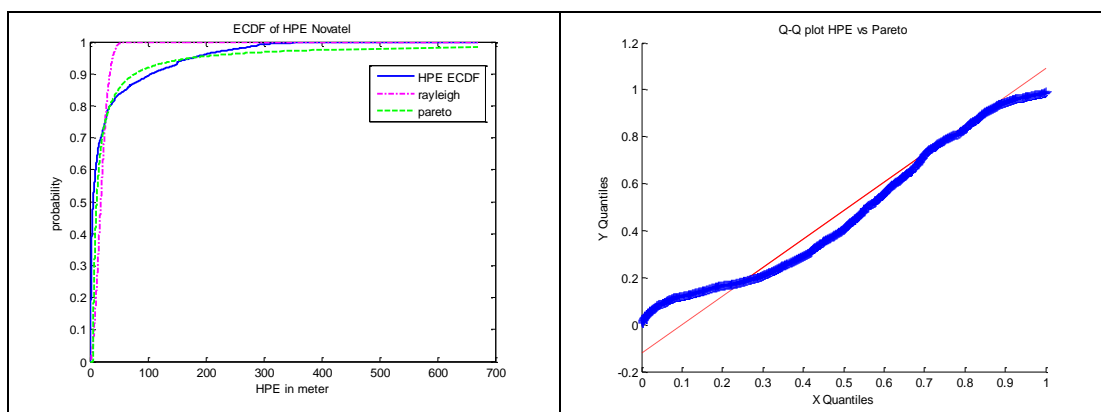


Figure 3d. CDFs and Q-Q Plot for Novatel receiver

5.2.3 Ublox 6T receiver

Good fitting of the HPE CDF with Pareto CDF in urban environment is also observed for the Ublox 6T receiver (Figure 3e).

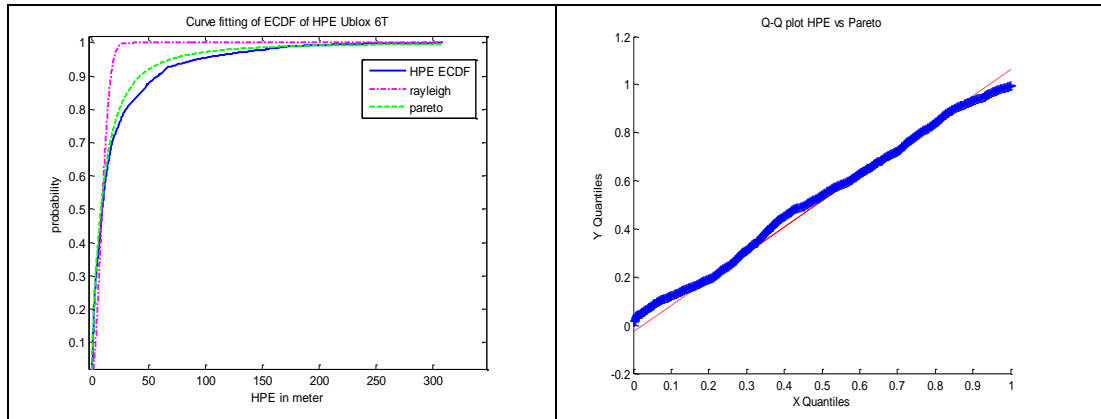


Figure 3e. CDFs and Q-Q Plot for Ublox 6T receiver

The observed results from the 3 receivers (Ublox 4T, Novatel, and Ublox 6T) suggest that generalized Pareto distribution is suitable to model the HPE distributions in urban environment. However, further validation is necessary with long data.

5.3 Curve fitting for along-track position errors and lateral position errors

Figure 4a shows the PDF of the along-track position errors and the lateral position errors in urban environment for Ublox 4T receiver. In this case, the position errors have both positive and negative value range. Generally, both PDFs have heavy tails as compared to standard Gaussian distribution as shown in Figure 4a.

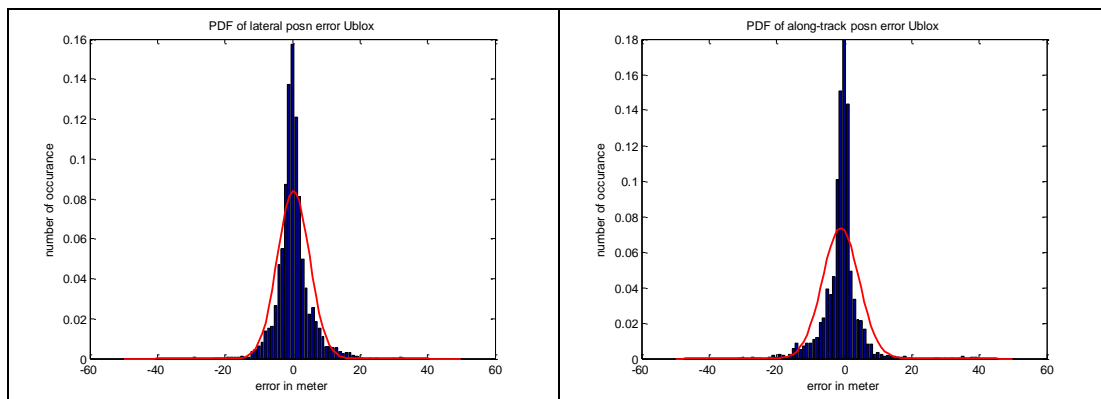


Figure 4a. PDFs of lateral and along-track position errors

In Figure 4b, their CDFs are fitted with a normal CDF, Student-T CDF and Pareto CDF for comparison. It can be seen that the Pareto has the best fit for both along-track error and lateral error CDFs.

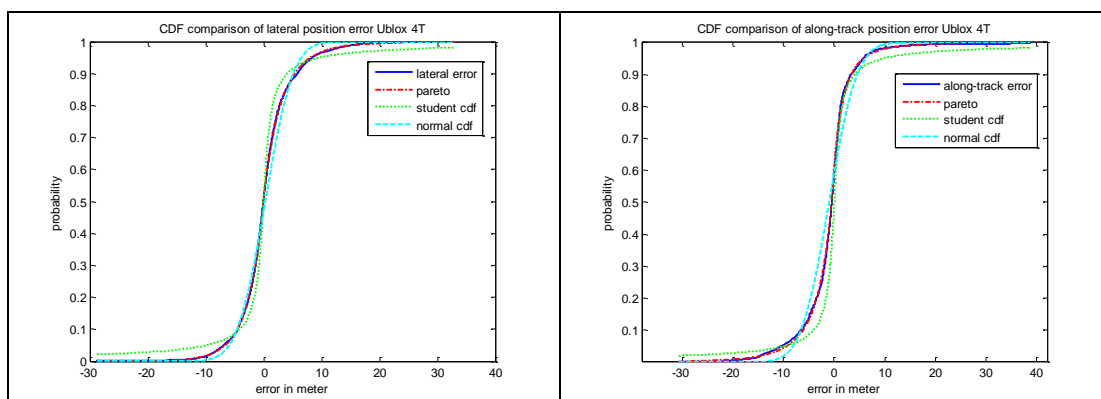


Figure 4b. CDF Curve fitting for lateral and along-track position errors for Ublox 4T receiver

Figure 4c and 4d below respectively show the lateral and along track errors of Novatel and Ublox 6T receivers that are being fitted by the Pareto distribution. From the plots, the GPD shows good fitting with the CDF of the lateral and along track errors.

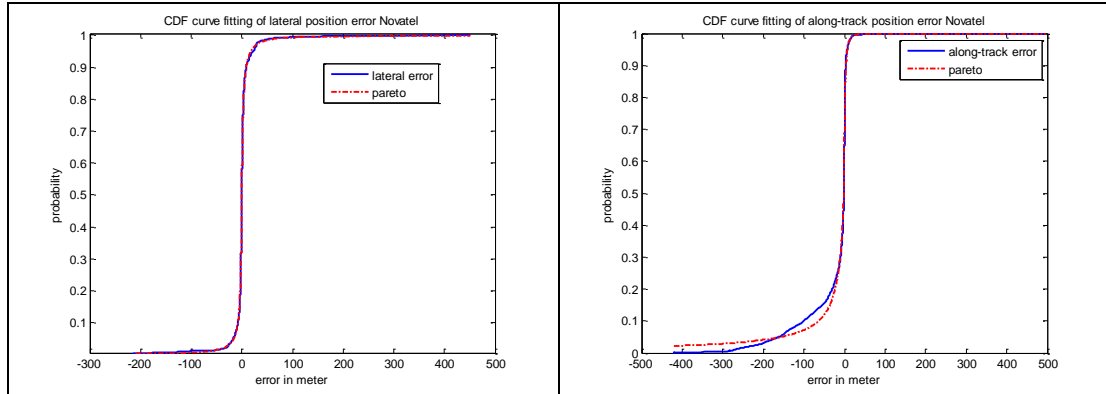


Figure 4c. CDF Curve fitting for lateral and along-track position errors for Novatel receiver

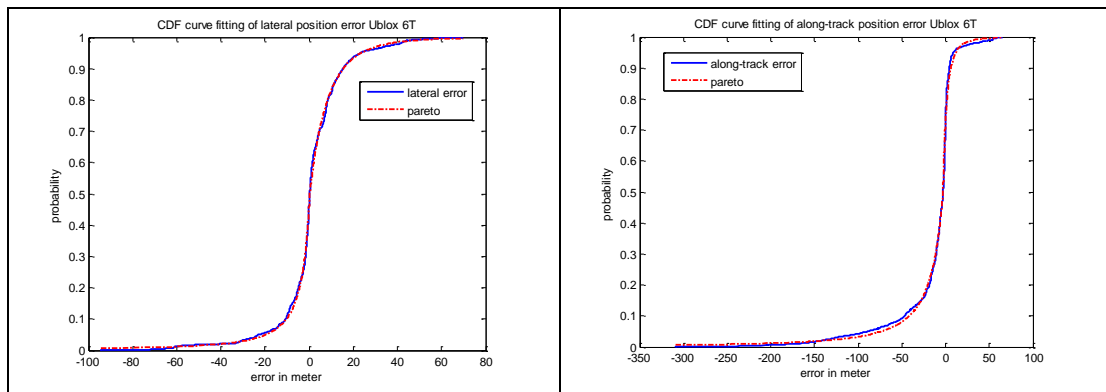


Figure 4d. CDF Curve fitting for lateral and along-track position errors for Ublox 6T receiver

Alternatively, the along-track and lateral position error could also be represented in their squared values. Figure 4e shows their CDF plots. In this form, their CDF can also be well fitted by the Pareto CDF as shown.

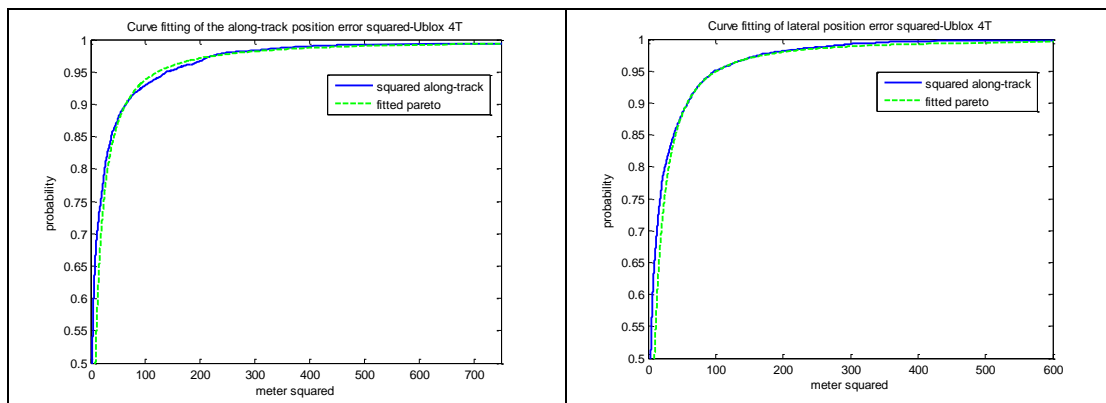


Figure 4e. CDF Curve fitting for along-track squared and lateral squared position errors

5.4 Overbounding HPE CDF by Pareto CDF

Figure 5 shows the overbounding of the HPE by the Pareto CDF for the case of Ublox 4T receiver. It can be seen that it complies with the CDF overbounding requirement. For the result in this experiment, the HPL for 90% integrity is 15 meters (HPE at 12 meters) and for 95% integrity is 20 meters (HPE at 15 meters). The tightness of the overbounding may be considered reasonable. While tighter overbound will improve availability in general, specific application requirements must also be taken into consideration especially for those which need ample safety distance.

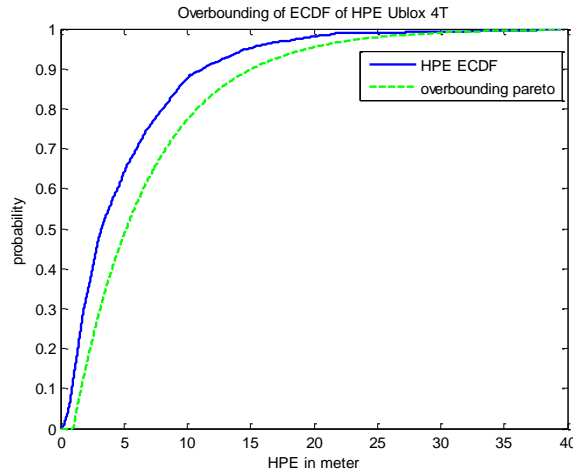


Figure 5. Overbounding of the HPE by Pareto distribution

5.4.1 Tail overbounding and curve fitting

The HPE CDF plots in Figure 3a, 3b and 3c also show that in the urban environments, the unwanted errors do not necessarily reside at the very ends of the tail of the distributions. Due to the biases that exist in the urban environments, the P_{HMI} is not so small for an acceptable value of alert limit (for example 10 meter). As opposed to the situation in the aviation sector, where one of the main issues of overbounding is sparse data at the tail of distribution, overbounding position errors in urban environment appears to not heavily implicated by the same issue.

Overall, the Pareto distribution seems to be able to fit the CDF of the position error quite well. However, it is not a perfect fit as can be seen in the results. This is expected because the distribution characteristic of position errors in the urban environment is very complex. Because of this, a parametric distribution will tend to face some limitation in modelling the position error distribution in the urban environment.

5.4.2 Direct position domain overbound vs range domain overbound

In obtaining the HPE CDF overbound, the direct position domain approach is able to bypass the difficulties and complexity of modelling the PR errors in urban environments that the range domain overbounding has to face. Nevertheless, there is a limitation in this direct position domain approach in that each satellite channel is not monitored. Therefore, even when enough satellites are available (for example 7 satellites), fault detection and exclusion (FDE) cannot be implemented using this approach. On the other hand, if the multiple biases of the measured PR combined with the geometry in such a way that the PRs residual remain small but the position error becomes large, only the position domain approach would detect the error and not in the range domain. A combination of both range-domain and position-domain approaches could be studied in order to benefit from their complementary positive aspects.

5.4.3 Classification of receiver performance

This exercise of characterizing position errors of the receivers in urban environment may also benefit the effort to categorize and certify the receivers. By having the HPE characteristics of the receivers, the receivers can be classified into several performance grades and this shall allow a proper selection of suitable receiver for a certain type of land application.

6 CONCLUSIONS

In this work, we considered the measurement bias in urban canyon that resulting in the non-Gaussian distributed position errors which challenge existing integrity monitoring methods. While the empirically based HPE distribution has a good fit with Rayleigh distribution in open sky environments, we observed that better fitting can be achieved using Pareto distribution in urban environments. Based on

the concept of direct position domain overbounding and CDF overbounding, the Pareto distribution was applied to overbound the HPE in the constrained conditions. In addition, the characterizations of the HPE also allow the classification or selection of the proper receiver for a certain application. Nevertheless, more data is needed to be processed to confirm that Pareto is a good model for positioning errors in urban canyons.

ACKNOWLEDGEMENTS

The authors would like to thank François Peyret from IFSTTAR and the BNAE working group for the fruitful exchange on the topic of GNSS integrity for road applications.

REFERENCES

Aichhorn K., Khalsa P., Seybold J. and Diani F. (2011). GNSS-based metering for vehicle applications and value added road services. 8th ITS European Congress 2011, Lyon, France.

Blanch J., Walter T. and Enge P. (2005). Protection level calculation in the presence of heavy tail errors using measurement residuals. Proc. of the European Navigation Conference GNSS (July 2005).

Cosmen-Schortmann J., Grush B., Hamilton C., Azaola-Sáenz M. and Martínez-Olagüe M. A. (2009). The need for standard performance definitions for GNSS road use metering. ITS World Congress, Stockholm, 2009.

DeCleene, B. (2000). Defining Pseudorange Integrity – Overbounding. Proceedings of ION GPS 2000. pp.1916-1924.

Giraud J., Mathieu M-L., Boyero Garrido J. P. and Fernandez Hernandez I. (2013). Pushing Standardisation of GNSS-based Location Systems to Support Terrestrial Applications Development. ION GNSS, Sept 2013.

Goldstein, H., Poole, C. and Safko, J. (2002) Classical Mechanics, 3rd Edition, San Francisco: Addison Wesley, 2002.

Groves, P. D., Jiang Z., Wang L. and Ziebart, M. K. (2012). Intelligent Urban Positioning using Multi-Constellation GNSS with 3D Mapping and NLOS Signal Detection. Proc. of the 25th International Technical Meeting ION GNSS'12, Nashville, September 2012, pp. 458-472.

Johnson, N. L., Kotz, S. and Balakrishnan, N. (1994). Continuous Univariate Distributions, Volume 1, second edition. New York: Wiley.

Langel, S., Khanafseh, S., and Pervan, B. (2012). Bounding Integrity Risk in the Presence of Parametric Time Correlation Uncertainty. Proceedings ION ITM 2012, Manassas, VA. pp. 1666-1680.

Lee, J., Pullen, S. and Enge, P. (2009) Sigma Overbounding using a Position Domain Method for the Local Area Augmentation of GPS. IEEE Transactions on Aerospace and Electronic Systems, vol.45, no.4, Oct. 2009, pp.1262-1274.

Lu M., Weavers K. and Van der Heijden, R. (2005). Technical feasibility of advanced driver assistance systems (ADAS) for road traffic safety. Transportation Planning and Technology, vol. 28, no. 3, pp. 167-187.

RTCA, (2006). Minimum Operational Performance Standards for Global Positioning System/ Wide Area augmentation system airborne equipment, RTCA – Washington DC, Document DO-229D, 2006.

Ober, P.B., de Haan, L., Li, D., van den Berg, A. and Farnworth, R. (2004). Statistical Validation Of SBAS Integrity. Proceedings of the European Navigation Conference GNSS 2004, 16 - 19 May 2004, Rotterdam, The Netherlands.

Osechas, O. and Rife, J. (2013). Tightening DGNSS Protection Levels Using Direct Position-Domain Bounding. Proceedings of ION GNSS+ 2013, Nashville, TN, September 2013, pp. 1329-1340.

- Rife, J. and Pullen, S.** (2005). The Impact of Measurement Biases on Availability for CAT III LAAS. NAVIGATION: Journal of the Institute of Navigation 2005-2006, vol.. 52, no. 4, pp. 215-228.
- Rife, J., Pullen, S., Pervan, B. and Enge, P.** (2004a). Paired overbounding and application to GPS augmentation. Position Location and Navigation Symposium, 2004. PLANS 2004. pp.439-446.
- Rife J., Walter T. and Blanch J.** (2004b). Overbounding SBAS and GBAS error distributions with excess-mass functions. Proc. International Symposium on GPS/GNSS, Sydney 6-8 Dec 2004.
- Rife, J., Pullen, S., Pervan, B. and Enge, P.** (2004c) Core Overbounding and its Implications for LAAS Integrity, Proceedings of ION GNSS 2004. pp. 2810-2821.
- Sayim, I., Pervan, B., Pullen, S. and Enge, P.** (2003). LAAS Ranging Error Overbound for Non-Zero Mean and Non-Gaussian Multipath Error Distributions. In Institute of Navigation: Proceedings of the ION Annual Meeting, Albuquerque, New Mexico, pp. 490-499.
- Shively, C. and Braff, R.** (2000). An overbound concept for pseudorange error from the LASS ground facility. Proceedings of IAIN World Congress/ION 55th Annual Meeting, San Diego, CA. June 26-28, 2000. pp. 661-671.
- Spangenberg, M., Calmettes, V., Julien, O., Tourneret, J.Y. and Duchateau, G.** (2008). Detection of variance changes and mean value jumps in measurement noise for multipath mitigation in urban navigation. 42nd Asilomar Conference on Signals, Systems and Computers, 2008, pp.1193-1197.
- Tiberius, C. and Odijk, D.** (2008). Does the HPL bound the HPE. In Proceedings of NaviTec'08 workshop. ESA-Estec, Noordwijk, The Netherlands, December 2008. pp. 10-12.
- Viandier, N., Nahimana, D.F., Marais, J. and Duflos, E.** (2008). GNSS Performance Enhancement in Urban Environment Based on Pseudo-Range Error Model. Position, Location and Navigation Symposium, 2008 IEEE/ION, 5-8 May 2008. pp.377-382.
- Walck, C.** (2007). Handbook on statistical distribution for experimentalists. Internal Report SUF-PFY/96-01, Stockholm. [<http://www.stat.rice.edu/~dobelman/textfiles/DistributionsHandbook.pdf>],p 139.
- Walter T., Blanch, J. and Rife, J.** (2004). Treatment of Biased Error Distributions in SBAS. Journal of Global Positioning Systems (2004), vol.3, No. 1-2, pp 265-272.